

# A Compact Single-Layer Dual-Band Microstrip Antenna for Satellite Applications

S. H. S. Esfahlani, A. Tavakoli, and P. Dehkoda

**Abstract**—In this letter, a compact single-layer, single-feed, dual-frequency microstrip antenna with a high frequency ratio is proposed. This antenna has a broadside and symmetrical radiation patterns suitable for space-borne applications. The prototype was fabricated on a Rogers RT/duroid 5880 substrate with a relative permittivity of 2.2 and thickness of 1.58 mm. The dual-band behavior is achieved by a shorting pin at 1.7–1.706 and 8.011–8.277 GHz with the frequency ratio of 4.75. In addition, the antenna is miniaturized by 46% compared to the conventional rectangular patch.

**Index Terms**—Compact microstrip antenna, high frequency ratio, multifrequency antenna, satellite applications.

## I. INTRODUCTION

MICROSTRIP antennas are popular because of their small size, low profile, light weight, flexibility, and their compatibility with integrated circuits [1]. Multiband microstrip antennas are in demand for many applications such as wireless local area network (WLAN) and satellite communications [2], [3]. Simple compact, lightweight, single-layer, dual-frequency microstrip antennas with a single feed and high frequency ratio are required in radar and communications systems such as synthetic aperture radars (SAR), dual-band GSM/DCS 1800 mobile communication systems, global positioning systems (GPS), and satellite communications.

Dual-frequency microstrip antennas could be categorized into multiresonator or reactive-loading antennas [4]. The former needs more than one radiating element such as multilayer stacked-patch antennas and multiresonator antenna in coplanar structures [5]. These structures are large, complex, and costly, thus they are not desirable for many applications. The latter uses a single radiating element with reactive loading for dual resonance where shorting pins and slot loading are among the popular methods [6]. Simplicity, low price and small size makes reactive loading desirable for dual-band antennas.

According to [4], the highest frequency ratio for a single-layer, single-feed, dual-frequency antenna is reported as 4.9 for the two resonant frequencies of 464 and 2276 MHz. The reported frequency ratio is suitable for satellite applications, but not in the desired remote sensing satellite allocated bands. Since

the design of a single-layer shared patch antenna for satellite applications is challenging, designers usually resort to multilayer structures [7]–[9].

L- and X-band frequencies of 1670–1710 MHz and 8.025–8.4 GHz are allocated for communication payloads of remote sensing satellites [9], and each satellite may use a portion of this allocation. For example, Meteosat works in the 1.698–1.709 and 8–8.4 GHz frequencies [10], using only 11 MHz of the first allocated frequency band. The needed frequency ratio for these bands is about 4.8. Achieving such a high ratio in a shared aperture in the desired frequency bands with a single feed and single layer is difficult and, thus, two resonating patches are most often used that make the antenna array large and heavy with complicated designs.

Here, reactive loading and shape deformation are used simultaneously to achieve a high frequency ratio. Initially, by shape deformation, two distinct patches are designed to resonate at each frequency band [11]. Then, using a shorting pin, the spurious harmonics between these two resonant frequencies are short-circuited, and a pure impedance match is obtained.

## II. ANTENNA DESIGN

The design procedure consists of three steps. First, two separate antennas at the desired frequency bands are designed. Second, they are connected by a bridge and a shorting pin. Finally, the design is tuned to the desired frequency bands by available commercial software.

### A. Patch Design and Shape Deformation

Here, a combination of a circle notched rectangular patch and a circular patch is used to achieve two distinct resonant frequencies as shown in Fig. 1(a). The circle notched rectangular patch is designed to resonate at 1.7 GHz [12], and the circular patch is designed to resonate at 8.2 GHz [1].

The dominant mode resonance frequency of a rectangular patch is

$$(f_r)_{010} = \frac{1}{2L_{\text{eff}}\sqrt{\epsilon_{\text{eff}}\sqrt{\mu_0\epsilon_0}}}$$

The rectangular patch with  $L = 58$  mm and  $W = 1.2$ ,  $L = 69$  mm is designed to resonate at 1.7 GHz. In order to consider the circular notch effect, the dimensions are further reduced by about 17%, leading to  $L = 48$  mm and  $W = 57$  mm [12].

The circular patch with  $R_{\text{in}}$  of 6.5 mm is designed to resonate in 8.14 GHz using the dominant mode resonance frequency

$$(f_r)_{110} = \frac{1}{2\pi\sqrt{\mu\epsilon_{\text{eff}}}} \left( \frac{\chi'_{11}}{a} \right)$$

Manuscript received August 01, 2011; accepted August 26, 2011. Date of publication September 06, 2011; date of current version September 22, 2011. This work was supported by Iran's Telecommunication Research Center (ITRC).

The authors are with the Department of Electrical Engineering, Amirkabir University of Technology, Tehran, Iran (e-mail: h-s-esfahlan@aut.ac.ir; tavakoli@aut.ac.ir; pdehkoda@aut.ac.ir).

Color versions of one or more of the figures in this letter are available online at <http://ieeexplore.ieee.org>.

Digital Object Identifier 10.1109/LAWP.2011.2167121

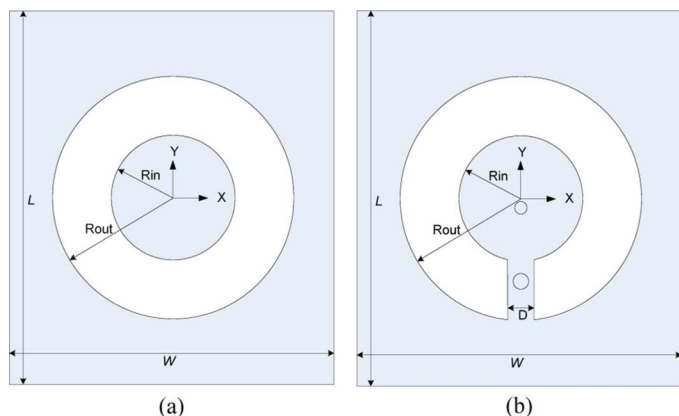


Fig. 1. (a) Primary design. (b) Proposed antenna.

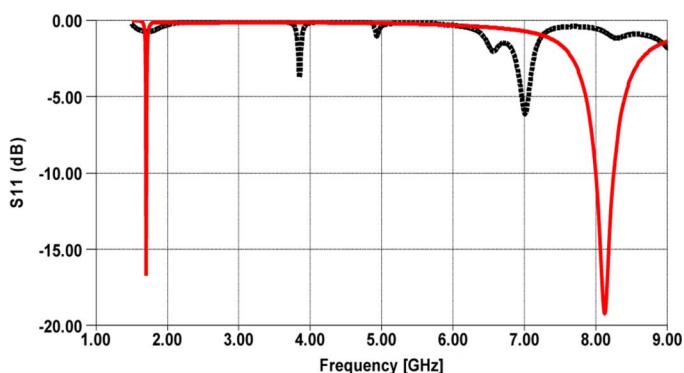


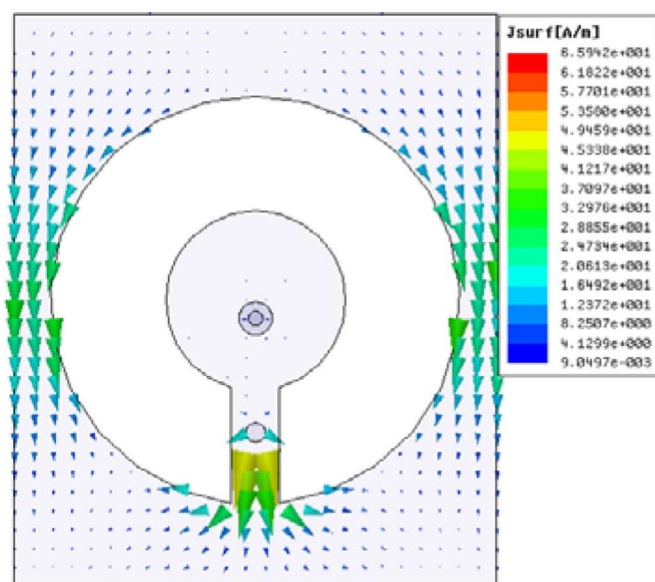
Fig. 2. Reflection coefficient of proposed design with inserting pin (solid line) and without inserting pin (dashed line).

where  $\chi'_{11}$  is the zero of the derivative of the first order Bessel function.  $R_{out}$  should be low enough to ensure an acceptable radiation pattern at the low frequency and high enough to reduce the coupling between the two resonant modes. Considering that  $R_{in} < R_{out} < W/2$ ,  $R_{out}$  is chosen to be 17 mm [12].

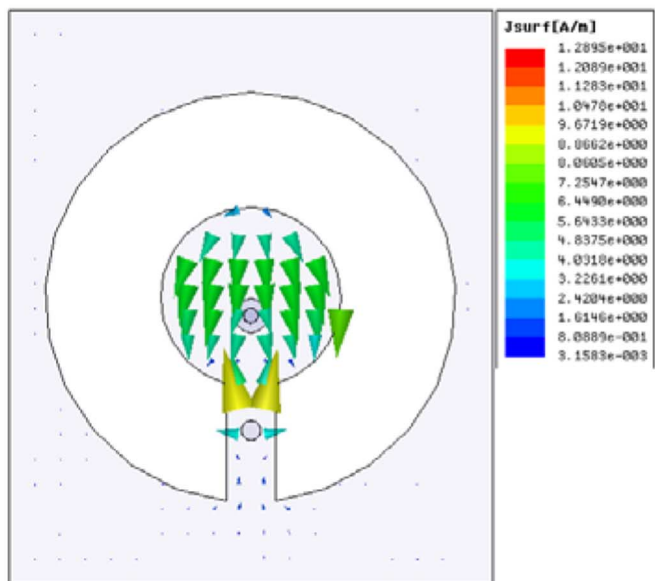
Since a feed location at the outer patch increases spurious resonances and adds harmonics that interfere with the upper resonance band [12], the feed should be inside the circular patch. In addition, a perfect impedance match at both frequency bands is obtained by an inner patch feed. Thus, for input impedance of  $50 \Omega$ ,  $X_{feed} = 0$  mm and  $Y_{feed} = 1.6$  mm [1]. Please note that all calculated parameters should finally be tuned for design accuracy.

### B. Reactive Loading Using Shorting Pin

As shown in Fig. 1(b), an interconnecting bridge links the inner and the outer patch. Furthermore, a shorting pin is inserted in the bridge between the two patches. Combination of the bridge and the shorting via works as a harmonic suppressor that short-circuits the spurious resonance currents and improves the impedance match. As depicted in Fig. 2, the proposed antenna without the pin has spurious resonances in between the two desired frequency bands, where they are all suppressed by the shorting pin and a pure match is obtained. Here, the shorting pin isolates low and high resonance regions from each other as depicted in Fig. 3.



(a)



(b)

Fig. 3. Patch current distribution at (a) 1.7 and (b) 8.14 GHz.

### C. Tuning

Finally, frequency deviations due to design alterations are adjusted by fine-tuning the design parameters. Adding a bridge and shorting via to the structure adds a spurious inductance and capacitance. Thus, their effects on resonant frequencies should be considered. By simulations, it is concluded that the inner patch should be enlarged due to the dominant inductive effect of the shorting via, and the outer patch is not noticeably affected because the inductive effect of shorting via is canceled by the capacitive effect of the bridge. Fig. 4 depicts the final design.

## III. RESULTS

The antenna of Fig. 4 is fabricated using Rogers RT/duroid 5880 substrate. The antenna performance is compared to a

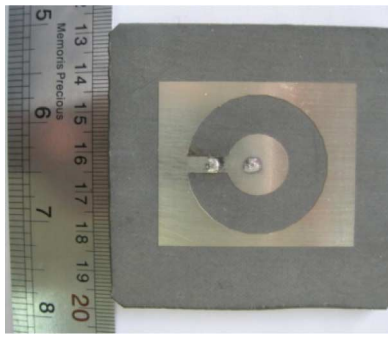


Fig. 4. Fabricated antenna with  $\epsilon_r = 2.2$ ,  $h = 1.58$  mm,  $R_{in} = 7.4$  mm,  $R_{out} = 17$  mm,  $L = 47.5$  mm,  $W = 40$  mm,  $D = 4$  mm,  $R_{pin} = 0.8$  mm,  $Y_{feed} = 1.5$  mm,  $Y_{pin} = 11$  mm.

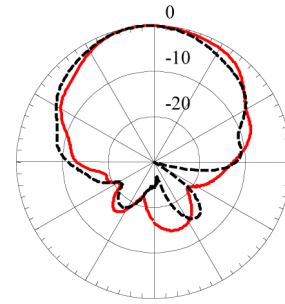


Fig. 6. Measured normalized radiation patterns at 1.7 GHz: E-plane (solid line) and H-plane (dashed line).

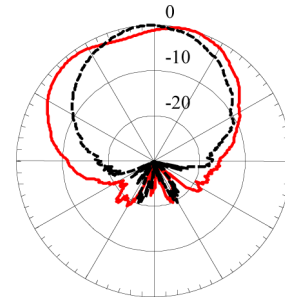


Fig. 7. Measured normalized radiation patterns at 8.088 GHz: E-plane (solid line) and H-plane (dashed line).

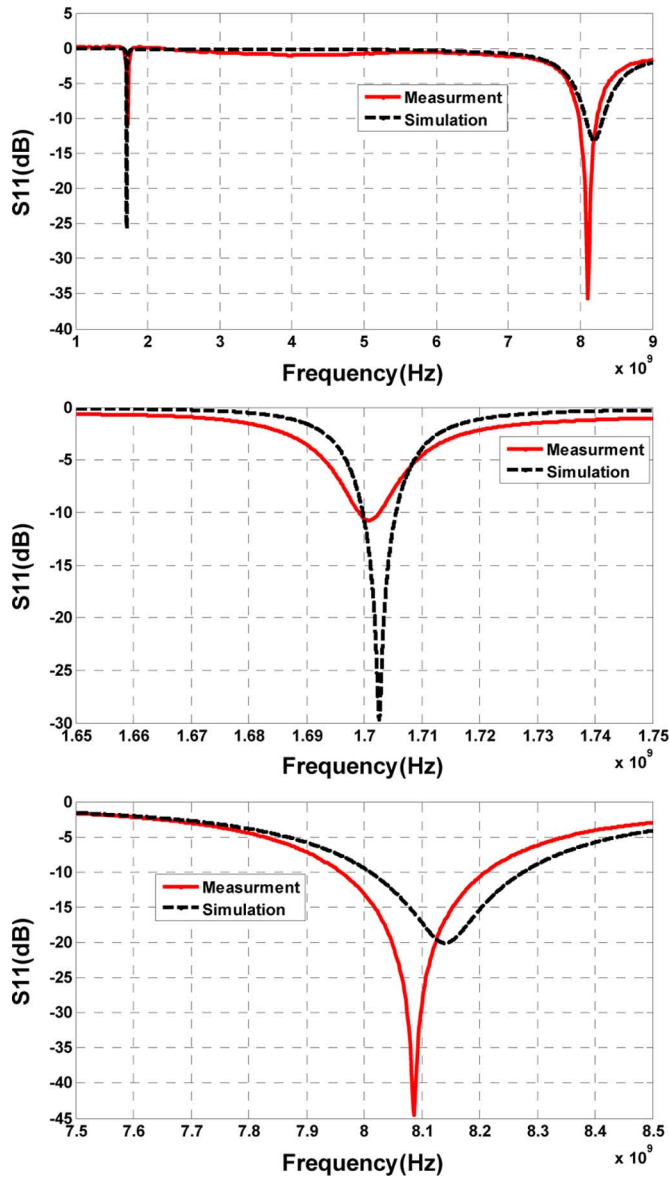


Fig. 5. Measured and simulated reflection coefficients.

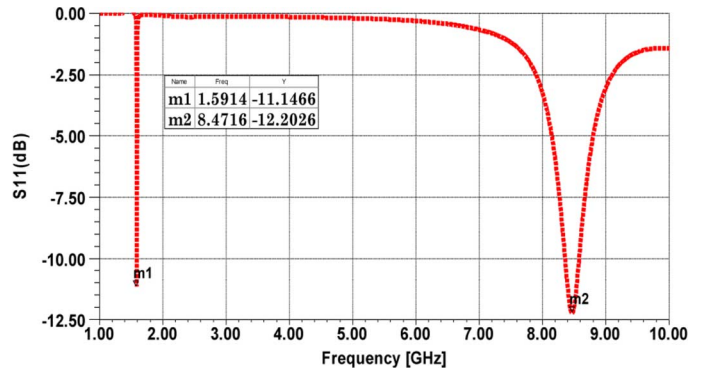


Fig. 8. Simulated reflection coefficient for the antenna with  $\epsilon_r = 2.2$ ,  $h = 1.58$  mm,  $R_{in} = 7$  mm,  $R_{out} = 19$  mm,  $L = 47.5$  mm,  $W = 40$  mm,  $D = 4$  mm,  $R_{pin} = 0.8$  mm,  $Y_{feed} = 1.85$  mm,  $Y_{pin} = 11.5$  mm.

commercially available finite-element-based software simulation. As shown in Fig. 5, the reflection coefficient results are in good agreement with each other, where the designed resonant

frequencies are 1.703 and 8.14 GHz, and the measured results are 1.701 and 8.088 GHz. The frequency shift is caused by the additional reactive load caused by the incomplete filling of the hole by the ribbon-like pin and coarse soldering. Similarly, the design bandwidths of 6 and 266 MHz were measured to be 4 and 250 MHz for lower and upper bands, respectively. The difference between measurement and simulation bandwidths is mainly due to the ribbon-like pin and incomplete filling of the hole.

Far-field radiation patterns were measured at 1.7 and 8.088 GHz. As shown in Fig. 6, the radiation patterns at 1.7 GHz are broadside and symmetrical, and the half-power beamwidths (HPBWs) are 78° and 76° for E- and H-planes, respectively. The upper-band radiation patterns are also broadside and symmetrical with HPBWs of 95° and 75° for the E- and H-plane, respectively, as depicted in Fig. 7. Symmetrical and broadside radiation patterns in both low and high frequency

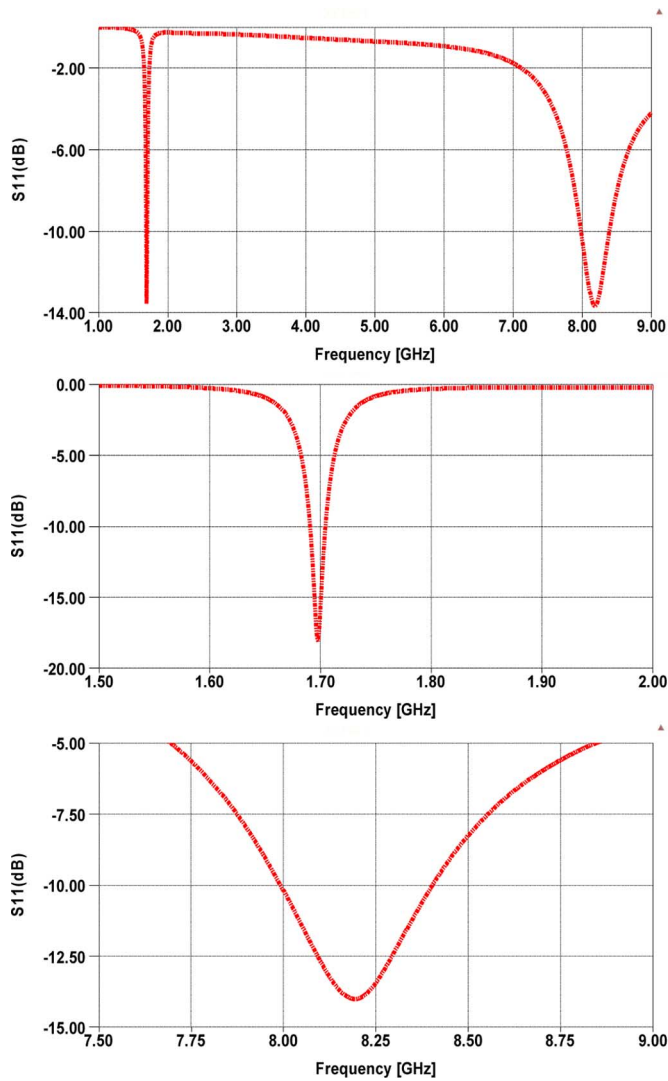


Fig. 9. Simulated reflection coefficient for the antenna with increased thickness and decreased dielectric constant.

bands are essential for illumination of a reflector dish or use as a single element of an array antenna. The design frequency ratio of 4.78 that is appropriate for satellite RS applications is in good agreement with the simulation result of 4.75. Moreover, the proposed patch is flexible in the sense of frequency ratio and bandwidth, meaning that by size reduction of the inner patch, increasing the radius of the circle notch, and changing the feed and pin locations, a frequency ratio of more than 5.3 (1.59 and 8.47 GHz) is achieved as shown in Fig. 8. Design parameters for this antenna are  $\epsilon_r = 2.2$ ,  $h = 1.58$  mm,  $R_{in} = 7$  mm,  $R_{out} = 19$  mm,  $L = 47.5$  mm,  $W = 40$  mm,  $D = 4$  mm,  $R_{pin} = 0.8$  mm,  $Y_{feed} = 1.85$  mm,  $Y_{pin} = 11.5$  mm.

Please note that a substrate with lower permittivity and higher thickness results in higher bandwidths. For example, as shown

in Fig. 9, a patch antenna of  $\epsilon_r = 1$ ,  $h = 2$  mm,  $R_{in} = 10.2$  mm,  $R_{out} = 22$  mm,  $L = 70$  mm,  $W = 60$  mm,  $D = 4$  mm,  $R_{pin} = 0.4$  mm,  $Y_{feed} = 4$  mm, and  $Y_{pin} = 17$  mm resonates at 1.69 GHz with a bandwidth of 14 MHz and at 8.17 GHz with the 410-MHz bandwidth. These bandwidths exceed the total allocated bandwidths of 11 and 400 MHz for remote-sensing satellite applications.

#### IV. CONCLUSION

A novel low-cost, compact, dual-band, single-feed, and single-layer microstrip antenna with a high frequency ratio and broadside and symmetrical radiation pattern is suggested. It is suitable for array designs or as a reflector feed in satellite applications. The simulation results and measurements are in good agreement with each other. Moreover, a frequency ratio of more than 5.3 is achieved by this design.

#### ACKNOWLEDGMENT

The authors would like to thank H. R. Karami, M. Rabbani, and I. Ahanian for their contributions.

#### REFERENCES

- [1] C. Balanis, *Antenna Theory, Analysis, and Design*, 2nd ed. New York: Wiley, 1997.
- [2] B. Li and K. W. Leung, "Dielectric-covered dual-slot antenna for dual band applications," *IEEE Trans. Antennas Propag.*, vol. 55, no. 6, pp. 1768–1773, Jun. 2007.
- [3] M. Ali, T. Sittironnarit, H. S. Hwang, R. A. Sadler, and G. J. Hayes, "Wideband/dual-band packaged antenna for 5–6 GHz WLAN application," *IEEE Trans. Antennas Propag.*, vol. 52, no. 2, pp. 610–615, Feb. 2004.
- [4] S.-C. Pan and K.-L. Wong, "Dual-frequency triangular microstrip antenna with a shorting pin," *IEEE Trans. Antennas Propag.*, vol. 45, no. 12, pp. 1889–1891, Dec. 1997.
- [5] J. Wang, R. Fralich, C. Wu, and J. Litva, "Multifunctional aperture-coupled stacked antenna," *Electron. Lett.*, vol. 26, no. 25, pp. 2067–2068, 1990.
- [6] R. B. Waterhouse and N. V. Shuley, "Dual frequency microstrip rectangular patches," *Electron. Lett.*, vol. 28, no. 7, pp. 606–607, 1992.
- [7] M. Pozar and S. D. Targonski, "A shared-aperture dual-band dual-polarized microstrip array," *IEEE Trans. Antennas Propag.*, vol. 49, pp. 150–157, Feb. 2001.
- [8] R. Pokuls, J. Uher, and D. M. Pozar, "Dual-frequency and dual-polarization microstrip antennas for SAR applications," *IEEE Trans. Antennas Propag.*, vol. 46, no. 9, pp. 1289–1296, Sep. 1998.
- [9] L. Shafai, W. Chamma, M. Barakat, C. Strickland, and G. Seguin, "Dual-band dual-polarized perforated microstrip antennas for SAR applications," *IEEE Trans. Antennas Propag.*, vol. 48, no. 1, pp. 58–66, Jan. 2000.
- [10] F. Ferrero, C. Luxey, G. Jacquemod, and R. Staraj, "Dual-band circularly polarized microstrip antenna for satellite application," *IEEE Antennas Wireless Propag. Lett.*, vol. 4, pp. 13–15, 2005.
- [11] S. C. Gao, L. W. Li, T. S. Yeo, and M. S. Leong, "A dual frequency compact microstrip patch antenna," *Radio Sci.*, vol. 36, no. 6, pp. 1669–1682, Nov.–Dec. 2001.
- [12] W. S. Chen, "Single-feed dual-frequency rectangular microstrip antenna with square slot," *Electron. Lett.*, vol. 34, no. 3, pp. 231–232, 1998.